Mechanism of Binding of Multivalent Immune Complexes to Fc Receptors. 1. Equilibrium Binding†

Steven K. Dower,* Charles DeLisi, Julie A. Titus,‡ and David M. Segal

ABSTRACT: The binding of two types of affinity cross-linked IgG oligomers to Fc receptors has been studied at 0 °C by using cells from the macrophage line, P388D_1. Dimers and trimers cross-linked with the bivalent affinity label, bis(2,4-dinitrophenyl)pimelic ester (BDPE), bind with increasing affinity as the oligomer size increases, give curved Scatchard plots, and deviate from stoichiometric binding. All of these features are consistent with a binding model in which oligomeric species, bound to Fc receptors by differing numbers of IgG subunits, are in equilibrium with solution-phase oligomer and with each other on the cell surface. A quantitative fit of binding and inhibition data was obtained by using a single monomer affinity constant of 1.3×10^6 M^{-1}, while the dimer and trimer binding data required two different sets of affinity constants; this heterogeneity in the multivalent interactions may arise from receptor clustering. Dimers and trimers cross-linked with the bivalent affinity label bis(α-bromoacetyl-ϵ-Dnp-Lys-Pro)ethylenediamine (DIBADL) are stable in solutions containing 10^{-4} M hapten but aggregate when hapten is removed. DIBADL oligomers give linear Scatchard plots when binding to P388D_1 cells in medium containing 10^{-4} M hapten; however, the Scatchard plots become more curved at higher hapten concentrations, eventually approaching those obtained from BDPE oligomers. These data show that DIBADL oligomers self-aggregate on the cell surface, presumably because they achieve high local concentrations when bound. Our analysis leads us to the conclusion that the cell surface receptor density is critical in determining the affinity of cells for multivalent ligands and that the affinity could be further modulated by receptor clustering and ligand self-aggregation.

Antibodies are biological adaptors which link a wide variety of foreign antigens with a small number of immune effector systems, e.g., complement or cellular effectors (Cathou & Dorrington, 1975; Beale & Feinstein, 1976; Winkelhake, 1978; Metzger, 1978). Antigen recognition occurs at the N-terminal, Fab, regions of antibody molecules, and antibody specificities are generated by variations in amino acid sequences in these regions (Hilschmann & Craig, 1965; Wu & Kabat, 1970). On the other hand, effectors bind to the C-terminal, Fc, regions of antibody molecules, all of which have the same amino acid sequence for antibodies of the same subclass. While antibodies with any particular specificity are normally present in low concentrations in blood, the total immunoglobulin concentration is high (10^{-4} M for IgG antibodies; Spiegelberg, 1974). Immune effectors, therefore, must be able to distinguish the Fc regions of small amounts of antigen-bound antibody from those of free immunoglobulins present at a much higher concentration.

The majority of evidence indicates that when antigens bind to IgG antibodies, it is the multivalency in Fc regions of the resulting complexes which enhances effector recognition (Metzger, 1974, 1978). The multivalency arises because antibodies are bivalent, and typical antigens are macromolecules which bear many determinants to which antibodies can bind. Consequently, immune complexes contain several molecules of both antigen and antibody cross-linked into a lattice (Nisonoff et al., 1975). Such complexes can provoke effector responses from several cell types, all of which bear specific cell surface receptors for the Fc region of IgG molecules (Boyden & Sorkin, 1960; Dickler, 1976). Among these cellular responses are endocytosis of the complex (Silverstein et al., 1977), exocytosis of various factors (Henson et al., 1972), lysis of antibody-coated cells (Moller, 1965; Cerottini & Brunner, 1974), and increased or decreased levels of antibody synthesis (Dennert, 1971; Morgan & Weigle, 1979; Parker et al., 1980). Immune complexes bind to cells bearing Fc receptors with much higher affinity than does monomeric immunoglobulin (Phillips-Quagliata et al., 1971; Dickler & Kunkel, 1972; Anderson & Grey, 1974; Leslie, 1980), and while several investigators have argued that this enhanced affinity derives from the multivalency of the complexes, many details of the binding remain unclear. We describe in this paper studies on a well-defined model system, the binding at 0 °C of affinity cross-linked oligomers of rabbit anti-Dnp[1] IgG antibodies to Fc receptors on cells from the mouse macrophage line, P388D_1. The analysis of data obtained with two types of model immune complexes (Segal & Hurwitz, 1976; Plotz et al., 1979) reveals several fundamental features of the binding of multivalent ligands to cell surface receptors, with implications for a wide range of cell surface receptor–ligand systems.

Experimental Procedures

Materials. Phosphate-buffered saline, pH 7.2 (PBS), glutamine, 0.02 M borate-buffered saline, pH 8.5 (BBS), Hanks' balanced salt solution (BSS), penicillin, and streptomycin were obtained from the National Institutes of Health media unit. RPMI 1640 and normal rabbit serum were purchased from Grand Island Biological Co. (Grand Island, NY). Fetal calf serum, purchased from Microbiological Associates (Walkersville, MD), was heat inactivated by incubating at 56 °C for 1 h before use. Bovine serum albumin (BSA) was purchased as lyophilized powder (bovine albumin, fraction V)

† From the Immunology Branch and Laboratory of Theoretical Biology, National Cancer Institute, National Institutes of Health, Bethesda, Maryland 20205. *Received March 26, 1981.*

‡ This paper represents partial fulfillment of the requirements for the degree of Doctor of Philosophy in the Department of Biochemistry, The George Washington University, Washington, DC.

[1] Abbreviations used: BBS, borate-buffered saline; BDPE, bis(2,4-dinitrophenyl)pimelic ester; BDPE oligomers, oligomers of anti-Dnp antibodies cross-linked with BDPE; BSA, bovine serum albumin; BSS, balanced salt solution; BSS medium, BSS containing 2.5% BSA and 0.2% sodium azide; DIBADL, bis(α-bromoacetyl-ϵ-Dnp-Lys-Pro)ethylenediamine; DIBADL oligomers, oligomers of anti-Dnp antibodies cross-linked with DIBADL; DMS, dimethylsuberimidate; Dnp, 2,4-dinitrophenyl; PBS, phosphate-buffered saline; $NaDodSO_4$, sodium dodecyl sulfate.

from Miles Laboratories. Chloramine T was purchased from Sigma Chemical Co. (St. Louis, MO). Dimethylsuberimidate dihydrochloride (DMS) was purchased from Pierce Chemical Co. (Rockville, IL). Sodium [^{51}Cr]chromate (1 mCi/mL, 8.1 μg of Cr/mL in sterile isotonic saline) was purchased from Amersham/Searle (Arlington Heights, IL), and sodium [^{125}I]iodide (17 Ci/mg) was purchased from New England Nuclear (Boston, MA). Bis(2-ethylhexyl) phthalate and dibutyl phthalate were from Eastman Chemicals (Rochester, NY).

Immunoglobulins. Monomeric nonimmune rabbit IgG was prepared from normal rabbit serum as described by Jones et al. (1979), and rabbit anti-Dnp antibodies were raised and isolated as described by Segal & Hurwitz (1977).

Preparation of Covalently Cross-Linked Oligomers. Nonimmune rabbit IgG was cross-linked with DMS (3-fold molar excess of DMS over protein; protein concentration ~100 mg/mL) as described previously (Segal & Titus, 1978). Rabbit anti-Dnp IgG was affinity cross-linked either with bis(α-bromoacetyl-ϵ-Dnp-Lys-Pro)ethylenediamine (DIBADL) (Segal & Hurwitz, 1976) or with bis(2,4-dinitrophenyl)pimelic ester (BDPE) (Plotz et al., 1979). Oligomers made with these reagents were purified by gel filtration (Segal & Hurwitz, 1977) and are termed DIBADL dimer and trimer or BDPE dimer and trimer, respectively. The BDPE oligomers were subjected to a second cycle of gel filtration to enhance size homogeneity. Radiolabeled dimer and trimer preparations were analyzed by polyacrylamide gel electrophoresis in sodium dodecyl sulfate ($NaDodSO_4$); the compositions are given in Table I.

Iodination. Proteins were iodinated by the chloramine T method, at molar ratios of approximately 1:1:1.5 protein/iodine/chloramine T (Segal & Hurwitz, 1977). In some control experiments, these conditions were varied.

$NaDodSO_4$–Polyacrylamide Gel Analysis of Radiolabeled Proteins. Oligomer composition was quantitated by $NaDodSO_4$–polyacrylamide gel electrophoresis of ^{125}I-labeled proteins using the conditions described by Segal & Hurwitz (1976). Approximately 10^4–10^5 cpm was applied to each channel of a Pharmacia PAA 2/16 slab gel. The gels were subjected to electrophoresis and stained, and individual tracks were sliced from botton to top at 2-mm intervals. Each slice was then counted for ^{125}I. For analysis of cell-bound proteins ~10^7 cells/mL were incubated with ^{125}I-labeled protein for 4 h at 0 °C in BSS medium (BSS containing 2.5% BSA and 0.2% sodium azide), washed twice, and lysed with 0.5% NP-40 in PBS. Nuclei were removed by centrifugation, and a sample of the supernatant containing 10^4–10^5 cpm was applied to a $NaDodSO_4$ gel. For analysis of dissociated protein, cells were equilibrated as described above, washed, and incubated in BSS medium for 1 h at 0 °C. The cells were then pelleted, and a sample of the supernatant was applied to the gel.

Cells. P388D_1 cells (Koren et al., 1975) were maintained in spinner culture, as described previously (Segal & Hurwitz, 1977). Cells were harvested, washed twice, and resuspended in BSS medium. The cells were chromium labeled by incubating 10^7–10^8 cells in 1–2 mL of BSS medium with 0.1 mL of stock sodium [^{51}Cr]chromate on ice for 5–10 min. They were then washed twice and resuspended for the binding assays in BSS medium at ~5×10^7 cells/mL.

Binding Assay. The binding of ^{125}I-labeled oligomers of IgG to ^{51}Cr-labeled P388D_1 cells was determined by incubating ~2×10^6 cells with oligomer in 200 μL of BSS medium on ice for 4–8 h. After equilibration, free oligomer was separated from cells and bound oligomer by centrifugation of triplicate 50-μL samples through phthalate oils (1.5 dibutyl phthalate–1 bis(2-ethylhexyl) phthalate v:v; Segal & Hurwitz, 1977). Nonspecific binding was determined at each concentration of ^{125}I-labeled protein by using samples containing a large (>25-fold) molar excess of DMS cross-linked oligomer or monomeric IgG at concentrations above 1.5 mg/mL. Specific binding was determined by subtracting the amount of label bound in the presence of the unlabeled protein (nonspecific binding) from the amount of label bound in its absence (total binding). Nonspecific binding, when plotted against the concentration of free, labeled protein, routinely gave a good fit to a straight line, intercepting the origin within two standard deviations. The nonspecific component was always <20% of the total, at the highest ligand concentration used.

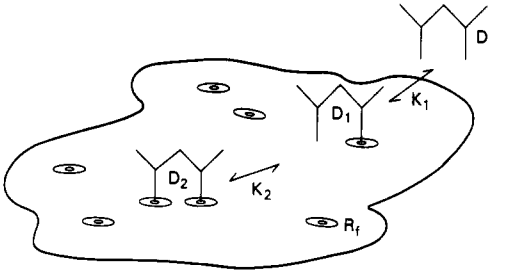

FIGURE 1: Schematic representation of binding of IgG dimers to cells bearing Fc receptors. According to the scheme, solution-phase dimer (concentration D, in molar units) binds to a free Fc receptor (concentration R_f, in cell surface concentration units) with an affinity constant K_1 (M^{-1}), giving rise to the monovalently bound intermediate (concentration D_1, in cell surface concentration units). The Fc receptors, which are assumed to be freely mobile in the membrane plane, bind the free subunit of D_1 with affinity K_2 [(cell surface units)$^{-1}$] to give the dimerically bound species (concentration D_2, in cell surface concentration units).

In experiments where the inhibition of binding of radiolabeled oligomer by unlabeled monomeric IgG was determined, cells were added to mixtures of the two proteins. The unlabeled monomeric protein was centrifuged for 1 h at 200000g immediately prior to the assay. The top half of the centrifuged solution was taken, and the protein concentration was determined from its absorbance at 280 nm.

Data Analysis. The average number of 7S immunoglobulin subunits bound per cell (r) was calculated from the ratio of ^{125}I to ^{51}Cr counts in the cell pellet as described previously (Jones et al., 1979). Data analysis and mathematical modeling were done by using MLAB, a mathematical modeling program written for the NIH Decsystem-10 time-sharing facility (Knott, 1979).

Theory

In this section we briefly discuss the model used in this paper to describe multivalent binding of IgG oligomers to Fc receptors. The mathematical description of the model is based on previously published treatments (Bell & DeLisi, 1974; DeLisi & Perelson, 1976; Dembo & Goldstein, 1978; Reynolds, 1979). The generalized equations used in the calculations are given in the Appendix.

Binding of Dimeric IgG to Cells. The mechanism of binding of a multivalent immune complex to a cell bearing Fc receptors is illustrated in Figure 1 for the simplest case, a dimer binding to receptors which diffuse freely in the membrane plane. The binding of a dimer occurs in two steps, described by the linked equilibria

$$D + R_f \rightleftharpoons D_1 \qquad K_1 = D_1/(2DR_f) \qquad (1A)$$

$$D_1 + R_f \rightleftharpoons D_2 \qquad K_2 = 2D_2/(D_1R_f) \qquad (1B)$$

where K_1 and K_2 are the associations constants for each step,

D is the free dimer concentration in bulk solution, D_1 is the local cell surface concentration of monomerically bound dimer, D_2 is the cell surface concentration of dimerically bound dimer, and R_f is the concentration of free receptor on the cell surface. All dimer species concentrations are expressed in terms of 7S IgG subunits. From eq 1A and 1B it follows that

$$D_1 = 2K_1DR_f \tag{2A}$$

$$D_2 = \tfrac{1}{2}K_2D_1R_f = K_1K_2DR_f^2 \tag{2B}$$

The factors of 2 and $^1/_2$ in eq 1 and 2 are statistical factors which arise because in the first step (eq 1A) the dimer can bind in either of two ways but can dissociate in one way, while in the second step the reverse is true. Dimer binding can be described by writing the expressions for the total concentration, R_0, of Fc receptors

$$R_0 = R_f + \tfrac{1}{2}D_1 + D_2 \tag{3A}$$

and the concentration, D_B, of bound dimer

$$D_B = D_1 + D_2 \tag{3B}$$

The factor of $^1/_2$ in the D_1 term of eq 3A arises because the two subunits of D_1 occupy only one receptor.

Substitution of the expressions for D_1 and D_2 (eq 2A and 2B) into eq 3A and 3B gives

$$R_0 = R_f + K_1DR_f + K_1K_2DR_f^2 \tag{4A}$$

$$D_B = 2K_1DR_f + K_1K_2DR_f^2 \tag{4B}$$

The quantity measured in binding experiments is r, the number of IgG subunits bound per cell

$$r = (D_B/R_0)r_0 \tag{5A}$$

where r_0 is the total number of receptors per cell.

If only monomeric binding occurs (i.e., if $K_2 = 0$), then eq 4A and 4B describe simple hyperbolic binding

$$r = \frac{2r_0K_1D}{1 + K_1D} \tag{5B}$$

In this case r is independent of R_f, the concentration of free receptor at the cell surface. In contrast, when dimeric binding occurs ($K_2 > 0$)

$$r = r_0K_1D\left[\frac{2 + K_2R_f}{1 + K_1D + K_1D(K_2R_f)}\right] \tag{5C}$$

and therefore dimer binding (and indeed any multivalent interaction) will depend upon R_f. In eq 5C the free receptor concentration appears in the product K_2R_f, and for an oligomer of any size, R_f will always appear in products of the form K_iR_f. This term, K_iR_f, is called the "enhancement factor" and is equivalent to the ratio of bound to free subunit for the binding of the ith subunit of an oligomer. Enhancement factors are dimensionless since K_i values are in reciprocal cell surface concentration units, and therefore estimates of cell surface concentrations are not required for interpreting oligomer binding data. The enhancement factors at low receptor occupancy, K_iR_0, and the number of receptors per cell, r_0, are the quantities which are estimated from binding experiments. While the cell surface concentration of receptors, R_0, cannot be estimated from binding experiments, R_0 is critical in determining the affinity of oligomers. For example, the effective binding constant for dimerically bound dimer, D_2, is $K_1(K_2R_f)$ (eq 2B). If R_0 were equivalent to 10^{-4} M (e.g., if 4×10^5 receptors were free to move in a 50-Å shell about a spherical cell of radius 8.5 μM) and K_2 equivalent to 3×10^5 M^{-1}, then K_2R_0 would be 30, and D_2 would bind with an affinity 30-fold greater than D_1, at low receptor occupancy.[2] At higher receptor occupancy K_2R_f would decrease, and the affinity of the cells for the dimer would drop.

In addition to enhancement factors, statistical factors will also modulate multivalent interactions. These factors depend upon both oligomer size and the binding step. For the ith step the statistical factor is equivalent to the number of ways in which the intermediate B_i can form from B_{i-1} divided by the number of ways in which the reverse reaction can occur. Thus, for the second step of dimer binding, the statistical factor is $^1/_2$ (eq 2B), whereas for the second step of trimer binding this factor is 1. Since the statistical factor for the first step (monovalent binding) is 2 for the dimer and 3 for the trimer, the final statistical factors for the second step are 1 and 3 for dimer and trimer, respectively. The general term for the statistical factor for the ith binding step of an oligomer of n subunits, $F_i^{(n)}$, is given by eq 10B in the Appendix.

Inhibition of Dimer Binding by Monomeric IgG. We can describe the inhibition of dimer binding by monomeric IgG by noting that bound monomer gives rise to an additional state of the receptors. The concentration of the receptor–monomer complex (M_1) is calculated from the equilibrium constant for the monomer–receptor interaction

$$M + R_f \overset{K_m}{\rightleftharpoons} M_1 \qquad M_1 = K_mR_fM \tag{6}$$

where M is the free monomer concentration and K_m is the monomer affinity constant. Equation 6 can be incorporated into eq 4A, giving

$$R_0 = R_f + K_1DR_f + K_mMR_f + K_1K_2DR_f^2 \tag{7}$$

Equations 7 and 4B describe the binding of dimer in the presence of monomer. Since both equations are quadratic in R_f, the inhibition of dimer binding by monomer cannot be described as simple competitive inhibition.

Self-Aggregation of Bound Ligand. Our data indicate that the DIBADL cross-linked IgG oligomers self-associate on the cell surface to form larger noncovalent complexes. In order to describe this effect mathematically, we have considered the case where cell-bound ligand molecules can associate with each other, with a binding constant K_s

$$L_1 + L_1 \overset{K_s}{\rightleftharpoons} L_2 \qquad L_2 = K_sL_1^2 \tag{8A}$$

$$L_2 + L_1 \overset{K_s}{\rightleftharpoons} L_3 \qquad L_3 = K_sL_1L_2 = K_s^2L_1^3 \tag{8B}$$

$$L_{j-1} + L_1 \overset{K_s}{\rightleftharpoons} L_j \qquad L_j = K_s^{j-1}L_1^j \tag{8C}$$

In our calculations, L_1 was determined from the oligomer binding equations, and the total binding was summed over several aggregation states, L_j. Only open linear aggregates were considered. In fact, calculations showed that it was not necessary to consider aggregates containing more than two oligomers. The equations used in the calculations are given in the Appendix. Recently, Perelson (1981) has published a more detailed analysis of self-aggregation.

[2] Note that the binding constant for D_2 cannot be obtained by multiplying K_1 by K_2, since the second binding step is linearly dependent upon the free receptor concentration. A binding constant of K_1K_2 for D_2 is obtained by adding the free energies of the individual binding steps (Sawyer & Windsor, 1976), but this ignores the substantial entropy loss when two receptor molecules are constrained to a small area of the cell surface by the bivalent ligand.

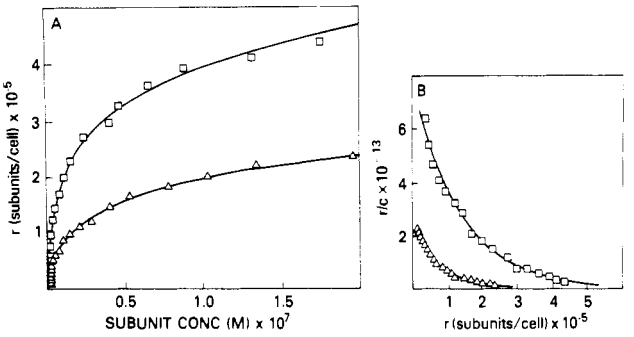

FIGURE 2: Binding of BDPE cross-linked dimer (△) and (□) trimer to P388D$_1$ cells at 0 °C. (A) Plot of the average number of IgG subunits bound per cell (r) vs. the free molar subunit concentration of solution-phase oligomer. (B) Data of (A) replotted in Scatchard form. All samples contained 3×10^6 cells. The nonspecific controls contained 6×10^{-6} M DMS cross-linked oligomer. Cell viability at the end of the experiment was 80% by trypan blue exclusion. The highest standard error of specific binding was 2.5%, calculated from triplicate samples. The curves shown in both panels were calculated from eq 11C–E by using the parameter values in Table II. Binding data were corrected for oligomer composition by using the data of Table I.

Table I: Composition of Affinity Cross-Linked Oligomers As Determined by NaDodSO$_4$–Polyacrylamide Gel Electrophoresis [a]

	L	M	D	T	H
DIBADL dimer [b]	9.1	19.4	79.0	1.8	0.0
DIBADL trimer [b]	11.6	14.9	19.5	54.8	0.0
BDPE dimer [b]	8.1	14.2	73.9	3.0	0.8
BDPE trimer [b]	7.4	6.3	4.9	73.5	7.8
cell bound [c] BDPE dimer	4.7	4.7	79.3	10.4	0.9
BDPE dimer [d] after dissociation from cells	3.9	6.5	84.2	4.6	0.9

[a] Values given in this table are integrated peak areas in percent total ^{125}I counts applied to the gel channel. L, M_r <150 000; M, M_r 150 000; D, M_r 300 000; T, M_r 450 000; H, M_r >450 000. [b] Oligomers were applied directly to gels. [c] Oligomers were bound to cells. After being washed, cells were lysed and spun and the lysates applied. [d] Cell-bound oligomer was allowed to elute from cells and was then applied to gels.

The important feature of a self associating system is that aggregation increases as the concentration of cell-bound ligand, L_1, increases (eq 8A–C). Since large aggregates will bind more avidly than smaller aggregates, the binding constant of a self-associating ligand will appear to increase as more and more ligand is bound. If the ligand is multivalent, this effect will tend to cancel the drop in affinity which arises from a depletion of free receptors.

Results and Discussion

Binding of BDPE Cross-Linked Dimer and Trimer to P388D$_1$ Cells—Simple Multivalent System. P388D$_1$ cells were incubated with radiolabeled BDPE oligomers at 0 °C, and the number of 7S subunits bound to the cell surface Fc receptors at equilibrium was measured by the phthalate oil separation technique. The results of a representative experiment, in which dimer and trimer binding were measured on the same cell preparation, are shown in Figure 2. NaDodSO$_4$–polyacrylamide gel analyses of either bound or released BDPE dimer showed that the dimer is neither degraded by nor covalently linked to the cells under these experimental conditions (Table I). Further, in the following paper we show that the uptake of dimer, at concentrations greater than 5×10^{-10} M, reaches equilibrium during the time of incubation (7 h) and that at least 85% of the bound material will dissociate from the cells [Dower et al. (1981), following paper in this issue]. The binding curves of Figure 2 therefore reflect true equilibria.

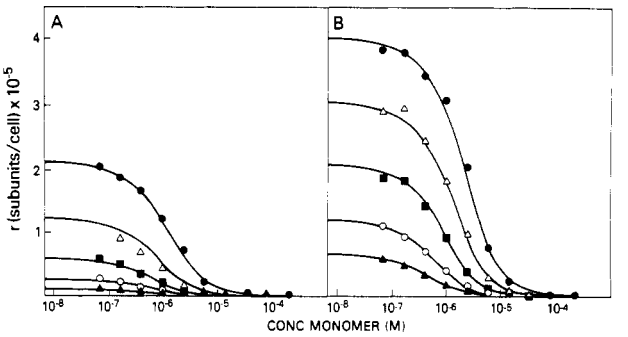

FIGURE 3: Inhibition of binding of BDPE cross-linked dimer and trimer to P388D$_1$ cells by monomeric, nonimmune IgG at 0 °C. (A) Inhibition of ^{125}I-labeled dimer binding. Inhibition was measured at (●) 1.83×10^{-7}, (△) 6.45×10^{-8}, (■), 2.24×10^{-8}, (○) 8.17×10^{-9}, and (▲) 3.14×10^{-9} M dimer (subunit concentrations). (B) Inhibition of ^{125}I-labeled trimer binding. Inhibition was measured at (●) 2.54×10^{-7}, (△) 8.64×10^{-8}, (■) 3.04×10^{-8}, (○) 1.02×10^{-8}, and (▲) 4.20×10^{-9} M ^{125}I-labeled trimer (subunit concentrations). The unlabeled monomer concentration was varied over an ~1000-fold range with 10 points of monomer concentration for each dimer or trimer concentration. Each sample contained 2.2×10^6 cells. The nonspecific controls contained 1.1×10^{-5} M DMS cross-linked oligomer. The samples were incubated on ice for 7 h, and the cell viability at the end of the experiment was 92% by trypan blue exclusion. The continuous curves in both panels are calculated from eq 11C–E by using parameter values similar to those in Table II. Binding data were corrected for oligomer composition by using the data of Table I.

The binding of radiolabeled monomeric IgG is too weak to be measured directly but can be detected by inhibition studies. Data presented in Figure 3 show that unlabeled monomeric IgG at concentrations greater than 10^{-5} M (1.5 mg/mL) completely inhibits the binding of both dimer and trimer to P388D$_1$ cells, over a wide range of oligomer concentrations. The monomeric IgG used in this experiment was fractionated by gel filtration and subsequently spun at 200000g for 1 h to ensure that contaminating aggregates were at minimal levels. The observed inhibition might still have been due to small amounts of contaminating aggregates or to heterogeneity in the monomeric IgG. However, absorbing monomeric IgG twice with P388D$_1$ cells at 0 °C (protein 1 mg/mL, cells 1×10^7 cells/mL) did not significantly reduce the monomer inhibition constant, suggesting that a high-affinity contaminant was not involved. The results of Figure 3 show that all receptors which bind oligomers also bind monomeric IgG and that the binding of monomeric IgG to the receptors is much weaker than dimer or trimer binding.

The data in Figures 2 and 3 show several qualitative features which are predicted by the model (Figure 1). First, the affinity of an oligomer for the cells increases as the size of the oligomer increases. This is shown by the Scatchard plots in Figure 2B where, for the same level of oligomer binding, the slope of the trimer curve is always greater than that of the dimer curve. According to the model, dimer would bind with a higher affinity than monomer, because the enhancement factor (K_2R_0) for the second step (eq 1B) is >2, thus stablizing D$_2$ with respect to D$_1$. Similarly, trimer would bind more tightly than dimer because a third such interaction could occur. In addition, statistical factors for any binding step increase with oligomer size; the statistical factor for dimeric binding of trimers is 3 times that for dimeric binding of dimers (see Theory). The distribution of bound intermediates will depend upon the products of enhancement and statistical (eq 10B) factors. In general, however, both factors will work to increase the avidity of binding with increased oligomer size.

Table II: Parameters for Binding of BDPE Dimer and Trimer and Monomeric IgG to P388D$_1$ Cells at 0 °C[a]

	site A	site B
K_1 (M^{-1})	$(1.3 \pm 0.5) \times 10^6$	[b]
K_2R_0	13.1 ± 2.0	207 ± 63
K_3R_0	2.5 ± 0.6	0 ± 1.2
r_0 (mol/cell)	$(2.1 \pm 0.2) \times 10^5$	$(0.9 \pm 0.1) \times 10^5$

[a] The parameter values were determined by least-squares fits to the data shown in Figures 2 and 3, with equations 11C-E. [b] Monomeric IgG binds with a single affinity.

Scatchard plots which are convex to the origin (Figure 2B) are a second characteristic feature of oligomer binding. Such curvature is predicted by the model developed here and is in agreement with a study previously published by DeLisi & Chabay (1979). The curvature in the Scatchard plots derives from decreases in enhancement factors (K_2R_f and K_3R_f) as free receptors become occupied by ligand. A third feature of the data in Figure 2 is that more IgG subunits bind to cells near saturation for trimers than for dimers, showing that not all trimer molecules bind by three subunits. This is also expected from the model (Figure 1) which predicts that multivalent binding will decrease with increased receptor occupancy.

Because the binding and inhibition data (Figure 2 and 3) show qualitative features expected of a multivalent system, we tested the model by least-squares fitting of eq 10E and 10F to the data. The overall fit of the theory to the data was good except at low ligand concentrations where more oligomer bound to the cells than could be explained by the simple multivalent model. We therefore considered the next simplest model, one in which the oligomers were bound multivalently by two types of receptors of differing affinities (eq 11C–E). For simplicity we have neglected states in which a single oligomer molecule binds to receptors of both types. Moreover, we have assumed that for both types of receptor, K_1 was the same for monomer, dimer, and trimer and the K_2R_0 was the same for dimer and trimer. With these constraints, an excellent fit was obtained to the data in Figures 2 and 3 when a minimum of seven parameters was varied. A less constrained fit using additional parameters would have given equally good agreement between theory and experiment, but it would not have been possible to estimate values for these additional parameters. The 12 curves drawn through the data in Figures 2 and 3 are calculated from this minimal model by using the best-fit parameter values given in Table II.

In order to test the significance of these results, we made simulations in which individual parameter values were held constant and the equations were fit to the data, allowing the other parameters to vary. These simulations showed that the parameters which could not be varied significantly from the "best-fit" values without losing agreement with the data were K_1 and $K_1K_2R_0$. In addition, K_3R_0 must be considerably less than K_2R_0 to obtain the relative amounts of dimer and trimer binding seen in Figure 2, and the number of receptors per cell, r_0, cannot be in error by more than a factor of 2. In summary, analysis of binding and inhibition data shows that monomeric IgG binds with a single affinity of 1.3×10^6 M^{-1}. Given the constraints described earlier, values for K_2R_0, K_3R_0, and r_0 are also obtained. These values show that the oligomers bind to about one-third of the receptors with higher affinity than the others and that there are an average of 3.0×10^5 receptors/cell. The analysis also shows that the enhancement factors decrease with oligomer size (Table II), suggesting that the third subunit of a trimer binds less tightly than the second subunit of a dimer. Finally, it should be emphasized that this quantitative fit does not mean that the model is a unique description of the system. However, the BDPE oligomers are multivalent, and it has been observed that Fc receptors can move in the plane of the plasma membrane (Dickler, 1976; Silverstein et al., 1977; Sulica et al., 1979; Michl et al., 1979). Therefore, the model provides a simple, rational description based on known properties of the system.

We have attributed the deviations from the simplest multivalent behavior to heterogeneity in the enhancement factors K_2R_0 and K_3R_0. Such heterogeneity does not arise from the iodination procedure since, in control experiments, dimer samples labeled over a 10-fold range in ^{125}I incorporation (by varying the amounts of either chloramine T or sodium [^{125}I]iodide) bound identically to cells from the same population. We have observed, however, variable degrees of heterogeneity with the same oligomer preparation and different cell samples (see, for example, Figure 4 in the following paper in this issue; Dower et al., 1981), suggesting that the heterogeneity is a property of the cells and not the oligomers. The affinity of oligomers for a cell is dependent on the cell surface receptor density, and flow microfluorometric analyses have shown that there is a moderately broad distribution of Fc receptor densities on P388D$_1$ cells (Titus et al., 1981). Therefore, heterogeneity in enhancement factors could conceivably arise from this variation in receptor density. However, detailed calculations, in which the population distribution was incorporated into a multivalent binding model with only one class of Fc receptors could not produce a fit to the data in Figure 2. The variation in receptor densities between cells of the same preparation is too limited to significantly affect the shape of the oligomer binding curves.

We have also considered the possibility that two types of Fc receptors of differing affinity for rabbit IgG could account for the observed heterogeneity in oligomer binding. Indeed P388D$_1$ cells do bind murine immunoglobulins of the IgG2a subclass with a somewhat higher (10-fold or less) affinity than proteins of the IgG1 or IgG2b subclasses (Unkeless & Eisen, 1975; Heusser et al.; 1977; Segal & Titus, 1978; Haeffner-Cavaillon et al., 1979), and many workers feel that IgG2a binds to a separate receptor. However, most (if not all) of rabbit IgG belongs to a single subclass (Mage et al., 1973), and rabbit IgG binds to P388D$_1$ cells with approximately the same affinity as murine IgG1 and IgG2b (Segal & Titus, 1978); there is no evidence either in the literature or in our own studies for two separate receptors with differing affinity for rabbit IgG. The observation (Table II) that monomeric rabbit IgG binds with a single affinity to P388D$_1$ cells makes it unlikely that heterogeneity in oligomer binding arises from two types of receptors. Rather, the most plausible explanation for heterogeneity in oligomer binding is that some of the Fc receptors are clustered. Clustered receptors would be at a higher local cell surface concentration than freely mobile ones, and, because K_2R_f and K_3R_f would be higher for these receptors, oligomers would bind to them preferentially. Ligand-induced receptor clustering is thought to be important in a number of biological systems (Goldstein et al., 1979). In a system such as ours, where the ligand is multivalent, preformed clusters could be important in modulating the affinity of the ligand for the cell.

Binding of DIBADL Cross-Linked Dimer and Trimer to P388D$_1$ Cells—Self-Aggregating System. Figure 4 shows the binding of DIBADL cross-linked dimer and trimer to P388D$_1$ cells at 0 °C in the presence of 10^{-4} M Dnp-ε-aminocaproate, under equilibrium conditions. These data show none of the

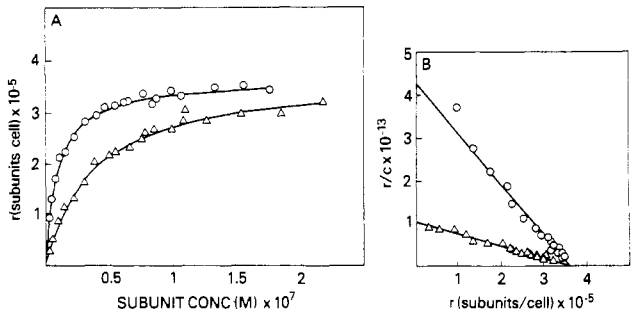

FIGURE 4: Binding of DIBADL dimer and trimer to P388D$_1$ cells at 0 °C. (A) Direct binding curves. (B) Scatchard plots. Dimer (△) and trimer (○) were equilibrated with P388D$_1$ cells on ice for 6 h in the presence of 10^{-4} M Dnp-ε-aminocaproate. Each sample contained 1.1×10^6 cells. Nonspecific binding was determined by using 8×10^{-6} M DMS cross-linked oligomer. Cell viability was 91% by trypan blue exclusion at the end of the experiment. Continuous curves in (A) and straight lines in (B) were calculated by using a simple biomolecular binding model and the parameters given in Table III. Binding data were corrected for oligomer composition by using the data of Table I.

Table III: Parameters for the Binding of DIBADL Dimer and Trimer to P388D$_1$ Cells at 0 °C[a]

	K ($M^{-1} \times 10^{-7}$)	r_0 (mol/cell $\times 10^{-5}$)
dimer	2.8 ± 0.2	3.67 ± 0.07
trimer	12 ± 1	3.62 ± 0.03

[a] The parameter values are derived from the data of Figure 4, by least-squares fits of a simple hyperbolic binding equation. The curves in Figure 4A and the straight lines in Figure 4B were calculated from the parameters given above.

complexities observed with the BDPE oligomers, confirming the earlier results of Segal & Hurwitz (1977). The Scatchard plots are linear for DIBADL dimer and trimer and extrapolate to the same intercept (Figure 4B, Table III), showing that the same number of subunits bind to the cells at saturation for both oligomers. In addition, the affinity of DIBADL oligomers appears to increase with size; DIBADL monomer does not bind significantly at the protein concentrations used in Figure 4, and the slope of the trimer plot is greater than that of the dimer.

It seemed probable to us that the deviation in binding behavior of the DIBADL cross-linked oligomers from that predicted for a simple multivalent system was due to self-aggregation on the cell surface. The DIBADL oligomers will aggregate in solution in the absence of Dnp-hapten (Segal & Hurwitz, 1976; Segal et al., 1979), presumably because these oligomers contain free combining sites and exposed haptenic groups which arise from DIBADL molecules bound covalently by only one BADL moiety. In support of this supposition, we observed that approximately half of a DIBADL dimer sample would bind to either a Dnp-Lys–Sepharose column or a sheep anti-Dnp IgG–Sepharose column, showing that DIBADL dimers do contain both free combining sites and exposed Dnp groups. The experiment shown in Figure 4 was done in the presence of a concentration of hapten (10^{-4} M) sufficient to prevent aggregation in solution. However, since the concentrations of bound oligomer on the cell surface could be very high (Cohen & Eisen, 1977; Reynolds, 1979), DIBADL oligomers might aggregate when bound, even in the presence of 10^{-4} M Dnp-ε-aminocaproate. We therefore measured the binding of DIBADL dimer to P388D$_1$ cells over a wide range of Dnp-hapten concentrations. The results, given in Figure 5, show that as the Dnp-hapten concentration is increased above 10^{-4} M, the Scatchard plots for DIBADL dimer binding gradually change from linear to the curved plots which are

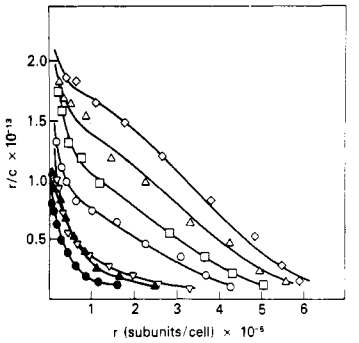

FIGURE 5: Effect of Dnp-ε-aminocaproate on the binding of DIBADL dimer to P388D$_1$ cells. DIBADL or BDPE dimers were incubated with cells on ice for 5 h with varying concentrations of Dnp-ε-aminocaproate. Dnp-ε-aminocaproate concentrations were 5.86×10^{-6} (◇), 2.35×10^{-5} (△), 9.4×10^{-5} (□), 2.35×10^{-4} (○), and 1.5×10^{-3} M (▽) for the DIBADL dimer and 5.86×10^{-6} (▲) and 1.5×10^{-3} M (●) for the BDPE dimer. Each sample contained 2.2×10^6 cells, and cell viability was 94% at the end of the experiment. Nonspecific binding was determined by using 5.5×10^{-5} M monomer. Data are plotted in Scatchard form. The continuous curves were calculated by using a two-site version of equations 13B and 13C, with parameters similar to those in Table II and a K_S value of 1.04×10^6 M^{-1}.

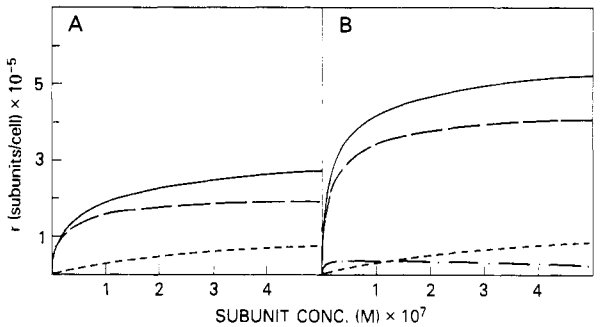

FIGURE 6: Calculated contribution of monomerically, dimerically, and trimerically bound states to total oligomer binding. (A) Dimer: (---) monomerically bound; (– – –) dimerically bound; (—) total bound. (B) Trimer: (---) monomerically bound; (– – –) dimerically bound; (–·–) trimerically bound; (—) total bound. The concentrations of the bound states were calculated from the parameter values in Table II by using eq 11C–E.

characteristic of the BDPE dimer. Dnp-hapten also had a small effect on the BDPE dimer binding in the experiment shown in Figure 5. This effect, the cause of which is unknown, is much smaller than the effect on the DIBADL dimer binding and in another experiment was not detected at all.

The data of Figure 5 suggest that Dnp–anti-Dnp-mediated self-aggregation plays a role in the binding of the DIBADL oligomers. Such self-aggregation should increase as the number of bound oligomer molecules increases, leading to the formation of larger, and therefore more tightly bound, complexes. With the P388D$_1$ cells, the enhanced affinity produced by self-aggregation of bound oligomer could cancel the fall in affinity expected for a nonaggregating multivalent system (e.g., as seen in Figure 2), thus producing linearity in the DIBADL oligomer Scatchard plots. In order to test whether this hypothesis was reasonable, we derived a model for IgG dimers which permits the formation of linear aggregates subsequent to binding to Fc receptors (Theory). Equations 13A–C are a mathematical description of this model. The best-fit curves calculated from these equations by using multivalent binding parameter values similar to those of Table II and a self-aggregation constant of 1.0×10^6 M^{-1} are shown in Figure 5. In order to produce the fit, it was necessary to set the concentration of monomerically bound intermediate, D_1, equal to 0 and to allow the total receptor number to in-

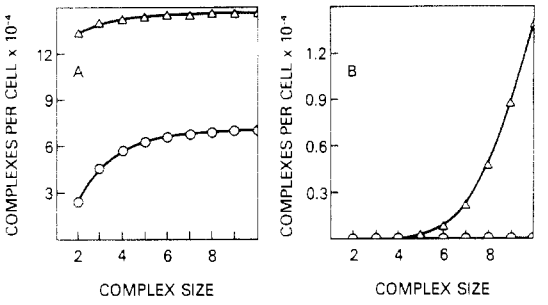

FIGURE 7: Calculated size dependence of the binding of 10^{-8} M immune complexes to cells bearing F_c receptors in the presence (B) and absence (A) of 10 mg/mL IgG. Calculated values for complexes bound per cell are plotted vs. the number of IgG molecules per complex for aggregating (Δ) and nonaggregating (O) complexes. Simulations were made by using the following parameter values: $r_0 = 3 \times 10^5$ molecules/cell, $K_1 = 1 \times 10^6$ M^{-1}, $K_2R_0 = 20$, $K_3R_0 = 4$, K_4R_0–$K_{10}R_0 = 1.1$, and $K_S = 2 \times 10^7$ M^{-1}. Equations 10F and 10G were used for the nonaggregating case and eq 13B and 13C for the aggregating case.

crease by 60% as the Dnp-hapten concentration was reduced to very low levels. Such an increase could arise, for example, from low amounts of dimer aggregation in solution at low hapten concentrations.

The quality of fit of the model to the data shown in Figure 5 suggests that self-aggregation is a reasonable explanation for the DIBADL oligomer binding data of Figures 4 and 5. The calculated curves are experimentally indistinguishable from linear. The observation that a satisfactory fit to the data of Figure 5 can be obtained only if the self-associating dimers are bound by both subunits suggests that self-association stabilizes divalent binding. The cause of this phenomenon is not clear. However, stabilization of fully multivalent binding would account for the observation that the dimer and trimer Scatchard plots extrapolate to the same value (Figure 4).

Distribution of Cell Surface Bound States—Predictions from Multivalent Binding Model. The parameter values in Table II were used to calculate the distribution of the bound oligomer among the different cell surface states (Figure 6). Neither BDPE dimer nor trimer binds fully multivalently over the concentration range indicated. One reason for this is that the enhancement factors K_2R_0 and K_3R_0 for the "site A" receptors are low, 13.1 and 2.5, respectively. In addition, statistical factors ($F_i^{(n)}$, eq 10B) destabilize full multivalent binding but enhance the affinity of intermediate states, an effect which increases with oligomer size. Since little of the BDPE trimer binds trimerically (Figure 6), we estimate that the enhanced affinity of trimer over dimer (Figure 2) is caused mainly by this statistical effect. We can also use the parameter values of Table II to estimate the molar concentration of Fc receptors on the cell surface. For example, if we assume that K_2 is the same as K_1, then R_0 would be 1×10^{-5} M for the major A site. However, the ratio of K_3R_0 to K_2R_0 for the major A site on P388D$_1$ cells is 0.19, showing that the average subunit receptor affinity constant is decreasing with increasing oligomer size. This ratio corresponds to 0.9 kcal/mol in loss of binding energy, which is a small fraction of the free energy of monomer binding (7.5 kcal/mole); possible causes of this effect have been discussed previously and include both entropic effects and steric hindrance of fully multivalent binding (Segal & Hurwitz, 1977). Assuming a similar ratio for K_2/K_1, R_0 would be $\sim 5 \times 10^{-5}$ M. On the other hand, the concentration of free hapten required to inhibit self-aggregation of DIBADL dimer by 50% is $\sim 1.5 \times 10^{-4}$ M. If free sites on the DIBADL oligomers bind hapten with the same affinity as the free Dnp groups associated with the oligomers, then the receptor concentration would be 1.5×10^{-4} M. Finally, the calculated concentration of 3×10^5 receptors/cell constrained in a 50-Å shell on a spherical cell surface of radius 8.5 μm (typical for P388D$_1$ cells) is 7.4×10^{-5} M. We therefore estimate that R_0 is in the range 10^{-5}–10^{-4} M.

Factors Governing the Fate of Immune Complexes in Vivo. In this section we consider the factors which might be important in modulating the binding of soluble immune complexes to cells bearing Fc receptors, in vivo. In the circulation the monomeric IgG concentration is fixed at $\sim 10^{-4}$ M. From the data shown in Figure 3, this is sufficient to completely inhibit the binding of BDPE dimer and trimer. Several features of the system could be changed in vivo to overcome this inhibition, i.e., cell surface receptor density, oligomer size, and (since natural immune complexes will have free determinants and combining sites) self-aggregation constants. It is unlikely that increases in cell surface receptor density could allow binding of such small complexes as dimer and trimer in vivo, since P388D$_1$ cells already have a relatively high receptor density (Titus et al., 1981) compared with natural hematopoietic Fc receptor-bearing cells. Therefore, the most probable factors which would allow soluble immune complexes to bind in vivo are initial size in solution and the propensity for self-aggregation on the cell surface. Accordingly, we have calculated the number of complexes that would be expected to bind to P388D$_1$ cells as a function of complex size for both aggregating and nonaggregating complexes (Figure 7), in the presence and absence of 10 mg/mL monomeric IgG. Values of the enhancement factors used were similar to those determined experimentally for the second and third binding steps and were 1.1 for all subsequent steps. Even if these values were in error, the qualitative features of Figure 7 would not be changed, since the major effect of size on binding in the nonaggregating case is that of the statistical factors $F_i^{(n)}$, which progressively enhance the early binding steps as the size increases. Figure 7B shows that, given the parameter values determined experimentally (Table II), even large nonaggregating complexes would not be expected to bind in the presence of 10 mg/mL IgG monomer. However, immune complexes give linear Scatchard plots when binding to Fc receptors (Leslie, 1980), suggesting that self-aggregation might occur in vivo. Our calculations predict that in a self-aggregating system with $K_s = 2 \times 10^7$ M^{-1} and at concentrations of immune complexes of ~ 1.5 μg/mL (a reasonable physiological value; Lambert et al., 1978; Theofilopoulos & Dixon, 1979; Cochrane & Koffler, 1973), significant binding will occur when a threshold size of 6 to 7 IgG molecules per complex is reached. As Figure 7A shows, in the absence of serum levels of IgG no such threshold exists, suggesting that circulating IgG could modulate the size threshold for complex binding.

The parameters used in the calculations for Figure 7 are based on those measured at 0 °C. It is known that the affinity constants of IgG for its receptor decrease with increasing temperature (Unkeless & Eisen, 1975; Segal & Hurwitz, 1977). We may have thus overestimated the inhibitory effect of serum levels of IgG. Finally, equilibrium binding only partially describes the interaction of monomeric IgG and immune complexes with cell surface Fc receptors. The kinetics of association and dissociation will also play a major role in the functioning of this system. We examine these in the following paper (Dower et al., 1981).

Acknowledgments

We thank Dr. Gary Knott for extensive help and advice on the application of MLAB to our system. We also thank Drs. Henry Metzger and Pierre Henkart for thoughtful suggestions

in the preparation of the manuscript.

Appendix

Multivalent Binding Mechanism—General Case. The model of dimer binding (eq 4A and 4B) can be generalized to any oligomer of n subunits. Let C be the subunit concentration of free oligomer, K_i the equilibrium constant for the ith step, R_f the cell surface concentration of receptors that are free, and R_0 the total receptor concentration. Equations have been cast in terms of R, the fraction of receptors that are free, in order to facilitate computations

$$R = R_f/R_0 \tag{9}$$

The cell surface concentration of an oligomer of n subunits bound by i subunits to receptors, $B_i^{(n)}$, can be written

$$B_i^{(n)} = R_0 F_i^{(n)} C \bar{K}_i R^i \tag{10A}$$

where

$$F_i^{(n)} = \frac{n!}{i!(n-i)!} \tag{10B}$$

and

$$\bar{K}_i = K_1 \prod_{j=2}^{i} K_j R_0 \tag{10C}$$

$B_i^{(n)}$ is the subunit concentration of the ith bound intermediate, in the same units as R_0. The total receptor concentration is

$$R_0 = R_f + \sum_{i=1}^{n} (i/n) B_i^{(n)} \tag{10D}$$

The "conservation" equation is thus

$$1 - R - \frac{1}{R_0 n} \sum_{i=1}^{n} i B_i^{(n)} = 0 \tag{10E}$$

and the total bound oligomer concentration $B_T^{(n)}$ is

$$B_T^{(n)} = \sum_{i=1}^{n} B_i^{(n)} \tag{10F}$$

Inhibition of oligomer binding by monomer can be described by incorporating eq 6 into eq 10E

$$1 - R(K_m M + 1) - \frac{1}{R_0 n} \sum_{i=1}^{n} i B_i^{(n)} = 0 \tag{10G}$$

Equations 10A–G also follow as a special case of previously developed theories (Gondolfi et al., 1978; DeLisi, 1980; Perelson, 1981).

Binding of Oligomers to Cells with Two Types of Fc Receptors. Assume that oligomer binding occurs to two types of Fc receptors, designated A and B. Then, by use of the same definitions as for a single type of receptor, the general terms for binding to each receptor can be written as

$$B_{iA}^{(n)} = R_{0A} [F_i^{(n)} C \bar{K}_{iA} R_A^i] \tag{11A}$$

$$B_{iB}^{(n)} = R_{0B} [F_i^{(n)} C \bar{K}_{iB} R_B^i] \tag{11B}$$

The conservation and binding equations for a two-site model are

$$1 - R_A(K_{mA} M + 1) - \frac{1}{n R_{0A}} \sum_{i=1}^{n} i B_{iA}^{(n)} = 0 \tag{11C}$$

$$1 - R_B(K_{mB} M + 1) - \frac{1}{n R_{0B}} \sum_{i=1}^{n} i B_{iB}^{(n)} = 0 \tag{11D}$$

$$B_T^{(n)} = \sum_{i=1}^{n} [B_{iA}^{(n)} + B_{iB}^{(n)}] \tag{11E}$$

Self-Aggregation of a Monovalent Ligand. In this section we consider the binding of a monovalent ligand to cell surface receptors, when the ligand can self-aggregate on the cell surface to form larger noncovalent complexes. Let L_1 be the cell surface concentration of unaggregated, bound ligand and K_S the ligand self-affinity constant. We assume that aggregation does not occur in the fluid phase; it only occurs on the cell surface. Further, we restrict the cell surface aggregation to the formation of open linear aggregates. We have shown in eq 8A–C (Theory) that the concentrations of a linear aggregate containing j molecules of L_1 is

$$L_j = K_S^{j-1} L_1^j \tag{12A}$$

Now, let

$$\bar{L}_1 = L_1/R_0 \tag{12B}$$

Then

$$L_j = R_0 (K_S R_0)^{j-1} \bar{L}_1^j \tag{12C}$$

and the total ligand bound (L_T) is

$$L_T = R_0 \sum_{j=1}^{m} j (K_S R_0)^{j-1} \bar{L}_1^j \tag{12D}$$

where m, the maximum possible aggregate size is equivalent to the number of receptors per cell. The conservation equation for such an aggregating system is

$$1 - R - \sum_{j=1}^{m} j (K_S R_0)^{j-1} \bar{L}_1^j = 0 \tag{12E}$$

Note that eq 12A or 12C gives the concentration in molecules of L_j. Hence, in calculating L_T in eq 12D, it is necessary to multiply L_j by j to calculate molecules of L bound to the cell surface.

Self-Aggregation on the Cell Surface of a Multivalent Ligand. Here we derive equations which describe the binding of a self-associating oligomeric ligand to a cell bearing receptors. Let $B_{ij}^{(n)}$ be the concentration of aggregates containing j oligomers each of n subunits, of which on average i are receptor bound. For simplicity we consider the special case in which i can only assume integral values in the range $1 \leq i \leq n$, that is, that all oligomers in the aggregate $B_{ij}^{(n)}$ are bound via i subunits. Then, substituting $B_i^{(n)}$ (eq 10A) for L_1 in eq 12A

$$B_{ij}^{(n)} = R_0 j (K_S R_0)^{j-1} [C F_i^{(n)} \bar{K}_i R^i]^j \tag{13A}$$

Thus, the binding is described by

$$B_T^{(n)} = \sum_{i=1}^{n} \sum_{j=1}^{m} B_{ij}^{(n)} \tag{13B}$$

and

$$1 - R - \sum_{i=1}^{n} \frac{1}{R_0 n} \sum_{j=1}^{m} i B_{ij}^{(n)} = 0 \tag{13C}$$

Equations 13B and 13C can be generalized for several classes of receptors and for inhibition by monomeric ligand.

References

Anderson, C. L., & Grey, H. M. (1974) *J. Exp. Med. 139*, 1175–1188.

Beale, D., & Feinstein, A. (1976) *Q. Rev. Biophys. 9*, 150–180.

Bell, G. I., & DeLisi, C. (1974) *Cell. Immunol. 10*, 415–435.

Boyden, S. V., & Sorkin, E. (1960) *Immunology 3*, 272–283.
Cathou, R. E., & Dorrington, K. (1975) *Biol. Macromol. 7*, 91.
Cerottini, J. C., & Brunner, K. T. (1974) *Adv. Immunol. 18*, 67–132.
Cochrane, C. G., & Koffler, D. (1973) *Adv. Immunol. 16*, 185–264.
Cohen, R. J., & Eisen, H. N. (1977) *Cell. Immunol. 32*, 1–9.
DeLisi, C. (1980) *Math. Biosci. 52*, 159–184.
DeLisi, C., & Perelson, A. (1976) *J. Theor. Biol. 62*, 159–210.
DeLisi, C., & Chabay, R. (1979) *Cell Biophys. 1*, 117–131.
Dembo, M., & Goldstein, B. (1978) *J. Immunol. 121*, 345–353.
Dennert, G. (1971) *J. Immunol. 106*, 951–955.
Dickler, H. B. (1976) *Adv. Immunol. 24*, 167–214.
Dickler, H. B., & Kunkel, H. G. (1972) *J. Exp. Med. 136*, 191–196.
Dower, S. K., Titus, J. A., DeLisi, C., & Segal, D. M. (1981) *Biochemistry* (following paper in this issue).
Goldstein, J. L., Anderson, R. G. W., & Brown, M. S. (1979) *Nature (London) 279*, 679–685.
Gondolfi, A., Giorenco, R. A., & Strom, A. (1978) *J. Theor. Biol. 74*, 513–527.
Haeffner-Cavaillon, N., Klein, M., & Dorrington, K. J. (1979) *J. Immunol. 123*, 1905–1913.
Henson, P. M., Johnson, H. B., & Spiegelberg, H. L. (1972) *J. Immunol. 109*, 1182–1192.
Heusser, C. H., Anderson, C. L., & Grey, H. M. (1977) *J. Exp. Med. 145*, 1316–1324.
Hilschman, N., & Craig, L. C. (1965) *Proc. Natl. Acad. Sci. U.S.A. 53*, 1403–1409.
Jones, J. F., Plotz, P. H., & Segal, D. M. (1979) *Mol. Immunol. 16*, 889–897.
Knott, G. D. (1979) *Comput. Programs Biomed. 10*, 271–280.
Koren, H. S., Handwerger, B. S., & Wunderlich, J. R. (1975) *J. Immunol. 114*, 894–897.
Lambert, P. H., Dixon, F. J., Zubler, R. H., Agnello, V., Cambiaso, C., Casali, P., Clark, J., Cowdery, J. S., McDuffie, F. C., Hay, F. G., McLennan, I. C. M., Masson, P., Muller-Eberhard, H. J., Peuttinen, K., Smith, M., Tappeniner, G., Theofilopoulos, A. N., & Verroust, P. (1978) *J. Clin. Lab. Immunol. 1*, 1–15.
Leslie, R. G. Q. (1980) *Eur. J. Immunol. 10*, 317–322.
Mage, R., Liebermann, R., Potter, M., & Terry, W. D. (1973) in *The Antigens* (Sela, M., Ed.) pp 299–376, Academic Press, New York.
Metzger, H. (1974) *Adv. Immunol. 18*, 169–207.
Metzger, H. (1978) *Contemp. Top. Mol. Immunol. 7*, 119–152.
Michl, J., Pieczonka, M. M., Unkeless, J. L., & Silverstein, S. C. (1979) *J. Exp. Med. 150*, 607–621.
Moller, E. (1965) *Science (Washington, D.C.) 147*, 873–879.
Morgan, E. L., & Weigle, W. O. (1979) *J. Exp. Med. 150*, 256–266.
Nisonoff, A., Hopper, J. E., & Spring, S. B. (1975) in *The Antibody Molecule*, Academic Press, New York, San Francisco, and London.
Parker, D. C., Wadsworth, D. C., & Schneider, G. B. (1980) *J. Exp. Med. 152*, 138–150.
Perelson, A. (1981) *Math. Biosci. 53*, 1–39.
Phillips-Quagliata, J. M., Levine, B. B., Quagliata, F., & Uhr, J. W. (1971) *J. Exp. Med. 133*, 589–601.
Plotz, P. H., Kimberly, R. P., Guyer, R. L., & Segal, D. M. (1979) *Mol. Immunol. 16*, 721–729.
Reynolds, J. A. (1979) *Biochemistry 18*, 264–269.
Sawyer, W. H., & Windsor, D. J. (1976) *Immunochemistry 13*, 141–147.
Segal, D. M., & Hurwitz, E. (1976) *Biochemistry 15*, 5253–5258.
Segal, D. M., & Hurwitz, E. (1977) *J. Immunol. 118*, 1338–1347.
Segal, D. M., & Titus, J. A. (1978) *J. Immunol. 120*, 1395–1403.
Segal, D. M., Guyer, R. L., & Plotz, P. H. (1979) *Biochemistry 18*, 1830–1835.
Silverstein, S. C., Steinman, R. M., & Cohn, Z. A. (1977) *Annu. Rev. Biochem. 46*, 669–722.
Spiegelberg, H. L. (1974) *Adv. Immunol. 19, 259*–294.
Sulica, A., Gherman, M., Medesan, C., Ghetie, V., & Sjoqvist, J. (1979) *Eur. J. Immunol. 9*, 985–990.
Theofipoulos, A. N., & Dixon, F. J. (1979) *Adv. Immunol. 28*, 89–189.
Titus, J. A., Sharrow, S. O., Connolly, J. M., & Segal, D. M. (1981) *Proc. Natl. Acad. Sci. U.S.A. 78*, 519–523.
Unkeless, J. C., & Eisen, H. N. (1975) *J. Exp. Med. 142*, 1520–1533.
Winkelhake, J. L. (1978) *Immunochemistry 15*, 695–714.
Wu, T. T., & Kabat, E. A. (1970) *J. Exp. Med. 132*, 211–250.